Journal of Magnetic Resonance **143,** 391–396 (2000)
doi:10.1006/jmre.1999.2010, available online at http://www.idealibrary.com on IDEAL®

Semi-Constant-Time HMSQC (SCT-HMSQC-HA) for the Measurement of $^3J_{H^NH^\alpha}$ Couplings in ^{15}N-Labeled Proteins

Helena Aitio and Perttu Permi[1]

NMR Laboratory, Institute of Biotechnology, P.O. Box 56, FIN-00014 University of Helsinki, Finland

Received October 8, 1999; revised December 20, 1999

A simple method for accurately measuring $^3J_{H^NH^\alpha}$ coupling constants in ^{15}N-labeled proteins is described. This semi-constant-time HMSQC-HA experiment combines the rapidity and convenience of the recently introduced CT-HMQC-HA scheme (Postingl and Otting, *J. Biomol. NMR* **12, 319–324 (1998)) with the high resolution and robustness of the HSQC experiment. The proposed method is demonstrated for the 76-residue human ubiquitin and** *Saccharopolyspora erythraea* **calerythrin (176 residues). Our results imply that the SCT-HMSQC-HA experiment is suitable also for proteins with less favorable NMR properties due to its good resolution and sensitivity.** © 2000 Academic Press

Key Words: **coupling constant; HSQC; CT-HMQC-HA; SCT-HMSQC-HA; NMR.**

Protein structure elucidation has long included the use of scalar three-bond couplings (*1*). These relatively small couplings, by means of their Karplus relationship (*2*), define the polypeptide ϕ, ψ, and χ dihedral angles. The determination of the dihedral angle ϕ, related to the three-bond coupling between $^1H^N$(i) and $^1H^\alpha$(i), has proven to be especially valuable in protein secondary structure elucidation. The numerous NMR pulse schemes developed for the measurement of the $^3J_{H^NH^\alpha}$ coupling can roughly be divided into four categories: *J*-resolved experiments (*3–6*), DQ/ZQ experiments (*7*), methods based on exclusive correlation spectroscopy (E.COSY) (*8–11*), and techniques utilizing quantitative *J*-correlation (*12–14*). The *J*-resolved experiments, from which the coupling is determined directly from in-phase or antiphase splitting, are usually not very suitable for larger proteins as the couplings to be measured are typically smaller than the proton resonance linewidths. Consequently, for larger proteins there is a need for methods which do not rely on the coupling to be measured. In the DQ/ZQ experiments the coupling constant of interest is extracted from large DQ and ZQ splittings. This approach is not prone to effects arising from differential relaxation of the in- and antiphase coherences, but multiple-quantum chemical shifts in the indirectly detected dimension complicate interpretation of the spectrum. The E.COSY-type experiments utilize a well-resolved ^1J coupling in one dimension for the measurement of a small, unresolved ^3J coupling in the other, orthogonal dimension. A drawback of the E.COSY-type experiments is that they create doublets in the spectrum and thus introduce unnecessary crowding. This resonance overlap can be alleviated by recording a three-dimensional spectrum. The experimental time is then, however, considerably longer. Very recently, Meissner *et al.* (*15*) showed that spin-state-selective filtering can be employed in the E.COSY-type experiments to reduce the spectral overlap in two-dimensional spectra. This approach necessitates an additional homonuclear mixing period, which is not very feasible for larger proteins due to the inefficiency of the TOCSY transfer and the spectral overlap of the NOESY spectra. More practical for larger proteins are experiments based on quantitative *J*-correlation; the coupling constants are extracted from the intensity ratio of a diagonal and a cross peak or of two cross peaks. As these experiments do not introduce additional cross peaks they have successfully been used for the determination of the $^3J_{H^NH^\alpha}$ couplings in larger proteins (*13, 14*). Still, even the well-established HNHA experiment may suffer from diagonal peak overlap in the F_2–F_3 plane despite its three dimensions.

Very recently, Ponstingl and Otting (*16*) introduced the CT-HMQC-HA and CT-HMQC-HN experiments which allow a very rapid and convenient measurement of the $^3J_{H^NH^\alpha}$ coupling constants from the familiar two-dimensional ^{15}N,^{1}H correlation spectrum by comparing cross peak intensities in two separate experiments. The constant-time nature of these experiments limits the resolution in the ^{15}N-dimension, though, and reduces their applicability for larger proteins.

In this Communication we propose a modification to the CT-HMQC-HA experiment which substantially improves the resolution in the ^{15}N-dimension. We refer to this new experiment as SCT-HMSQC-HA as in this semi-constant-time experiment one part of the ^{15}N chemical shift evolution is acquired under ^{15}N–^{1}H multiple-quantum coherence and the other part under ^{15}N single-quantum coherence. This new method allows an accurate and rapid measurement of the $^3J_{H^NH^\alpha}$ couplings in ^{15}N-labeled protein samples with high sensitivity and resolution.

The basic principle of the pulse scheme (Fig. 1) is the same

[1] To whom correspondence should be addressed. Fax: +358 9 191 59541. E-mail: Perttu.Permi@helsinki.fi.

1090-7807/00 $35.00

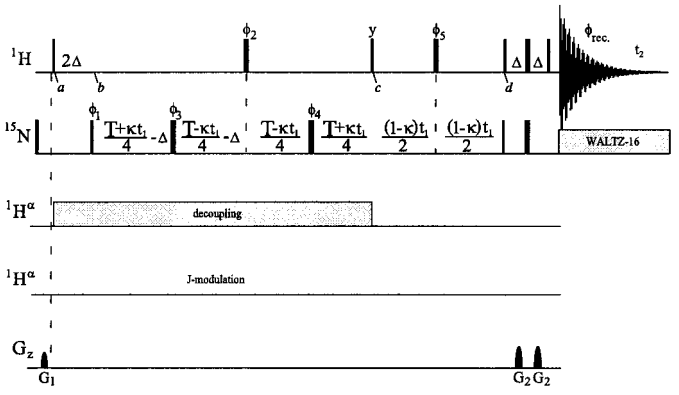

FIG. 1. Pulse scheme of the SCT-HMSQC-HA experiment. Narrow and wide rectangular pulses denote 90° and 180° flip angles, respectively. The reference spectrum is recorded by applying semi-selective decoupling to $^1H^\alpha$ region between time periods a and c. The attenuated *J*-modulated spectrum is recorded by omitting this $^1H^\alpha$-decoupling. Time period *T*, extending from point a to c, can be chosen freely, but is usually 20–70 ms, depending on the size of the expected coupling constants and the rotational correlation time of the molecule. Delay durations: $\Delta = 1/(4J_{HN})$, $0 \le \kappa \le (T - 4\Delta)/t_{1,max}$. Phase cycling: $\phi_1 = x, -x$; $\phi_2 = 2(x), 2(y), 2(-x), 2(-y)$; $\phi_3 = 8(x), 8(y)$; $\phi_4 = 16(x), 16(y)$; $\phi_5 = 32(x), 32(-x)$; $\phi_{rec} = 2(x, -x, -x, x), 4(-x, x, x, -x), 2(x, -x, -x, x)$. Frequency discrimination in F_1 dimension is obtained by altering the phase ϕ_1 according to the States–TPPI protocol (*22*). All gradients are 1 ms long with strengths $G_{1,2} = 12, 19$ G/cm. The semi-selective decoupling field was applied to $^1H^\alpha$-region (5.2–3.2 ppm) by using the off-resonance G3 pulse cascade (*23*), generated with Pbox software (*24*). More sophisticated selective $^1H^\alpha$-decoupling schemes (*16*) with better excitation profiles compared to the G3-shape can be used as well for better selectivity. It might also be advantageous to apply decoupling far off-resonance in the *J*-modulated experiment for more comparable heating and Bloch–Siegert shifts between the two experiments. The water suppression was achieved by the WET scheme (*25*) prior to the actual pulse sequence.

as that in the CT-HMQC-HA experiment (*16*). Two experiments are thus recorded: in one experiment the semi-selective proton decoupling is applied to the α-proton region, whereas in the other the amide proton is allowed to couple with the α-proton. This results in two ^{15}N,^{1}H correlation spectra with different ^{15}N,^{1}H cross-peak intensities. The experimental $^3J_{H^NH^\alpha}$ couplings can be extracted from the intensity ratio of the cross peaks in the decoupled and *J*-modulated experiments:

$$\cos(\pi JT) = I_m/I_{dec}, \qquad [1]$$

where I_m and I_{dec} are the intensities of the *J*-modulated and the decoupled cross peak, respectively, and *T* is the delay used for the *J*-modulation.

The semi-constant-time SCT-HMSQC-HA experiment is a combination of the constant-time HMQC and the HSQC schemes. Initially, heteronuclear multiple-quantum coherence, described by the density operator $H_x^N N_y$, is created in the usual HMQC manner (time point b). This is advantageous especially to larger proteins as the ^{15}N–^{1}H multiple-quantum coherence relaxes more slowly than the proton single-quantum coherence in the slow molecular tumbling limit (*4*). Subsequently, the ^{15}N chemical shift evolution takes place in a semi-constant-time manner between the time points b and d. One part of the ^{15}N chemical shift evolves under multiple-quantum coherence (time points b to c). The other part evolves under antiphase ^{15}N single-quantum coherence $H_z^N N_y$ (time points c to d), generated by the 90°(^{1}H) pulse at time point c. The relaxation rate of the antiphase single-quantum coherence is usually smaller than that of the ^{15}N–^{1}H multiple-quantum coherence; therefore, it is beneficial to develop one part of the ^{15}N chemical shift under ^{15}N single-quantum coherence. The following reverse INEPT step is used to transfer magnetization from the nitrogen back to the amide proton as in the usual HSQC experiment. The final 90°(^{1}H) pulse prior to the acquisition period is used to purge any undesired magnetization. The semi-selective decoupling is applied (or is absent in the *J*-modulated experiment) between time points a and c. At the end of the pulse sequence the observable magnetization at the amide proton frequency is proportional to $H_x^N \cos(\omega_N t_1)$ in the decoupled experiment and to $H_x^N \cos(\pi JT)\cos(\omega_N t_1)$ in the *J*-modulated experiment. In the *J*-modulated experiment the signal intensity is attenuated by $\cos(\pi JT)$ and, as *T* is known, $^3J_{H^NH^\alpha}$ can be calculated from Eq. [1].

The time periods for the *J*-modulation and the ^{15}N chemical shift evolution can be chosen independently, ensuring that the resolution in the F_1 dimension is not restricted by the length of the *J*-modulation period and vice versa. In order to obtain a sufficient resolution in the two-dimensional spectrum, a t_1-acquisition time larger than 30–40 ms is needed. Although *J*-modulation and ^{15}N chemical shift evolution periods can be separated to obtain high resolution (*17*), this approach becomes insensitive when protein size increases. An optimal resolution and sensitivity, even for larger proteins with faster transverse relaxation, is achieved by means of a semi-constant-time evolution period for the ^{15}N chemical shift. In that way, a major part of the *J*-modulation period is used for the ^{15}N frequency labeling under ^{15}N–^{1}H multiple-quantum coherence. Additionally, part of the ^{15}N chemical shift evolves under ^{15}N single-quantum coherence as in the usual HSQC experiment. It is noteworthy that the 90°(^{1}H) at time point c pulse converts the undesirable $H_y^N N_y H_z^\alpha$ coherence into a triple-quantum $H_y^N N_y H_x^\alpha$ coherence, which will not get converted to observable magnetization at amide proton frequency prior to the acquisition period. The pulsed field gradient sensitivity-enhanced scheme (*18*) would convert part of the $H_y^N N_y H_x^\alpha$ magnetization to observable magnetization at $^1H^N$-frequency of the *J*-modulated experiment and thus distort the coupling constant values. Hence, the sensitivity-enhancement scheme was not implemented in this sequence.

The accuracy of the SCT-HMSQC-HA experiment was evaluated by comparing the experimental $^3J_{H^NH^\alpha}$ couplings to those obtained with the CT-HMQC-HA scheme using human ubiquitin, a small 8.6-kDa (76 amino acid residues) protein that has intensively been investigated by NMR spectroscopy. The

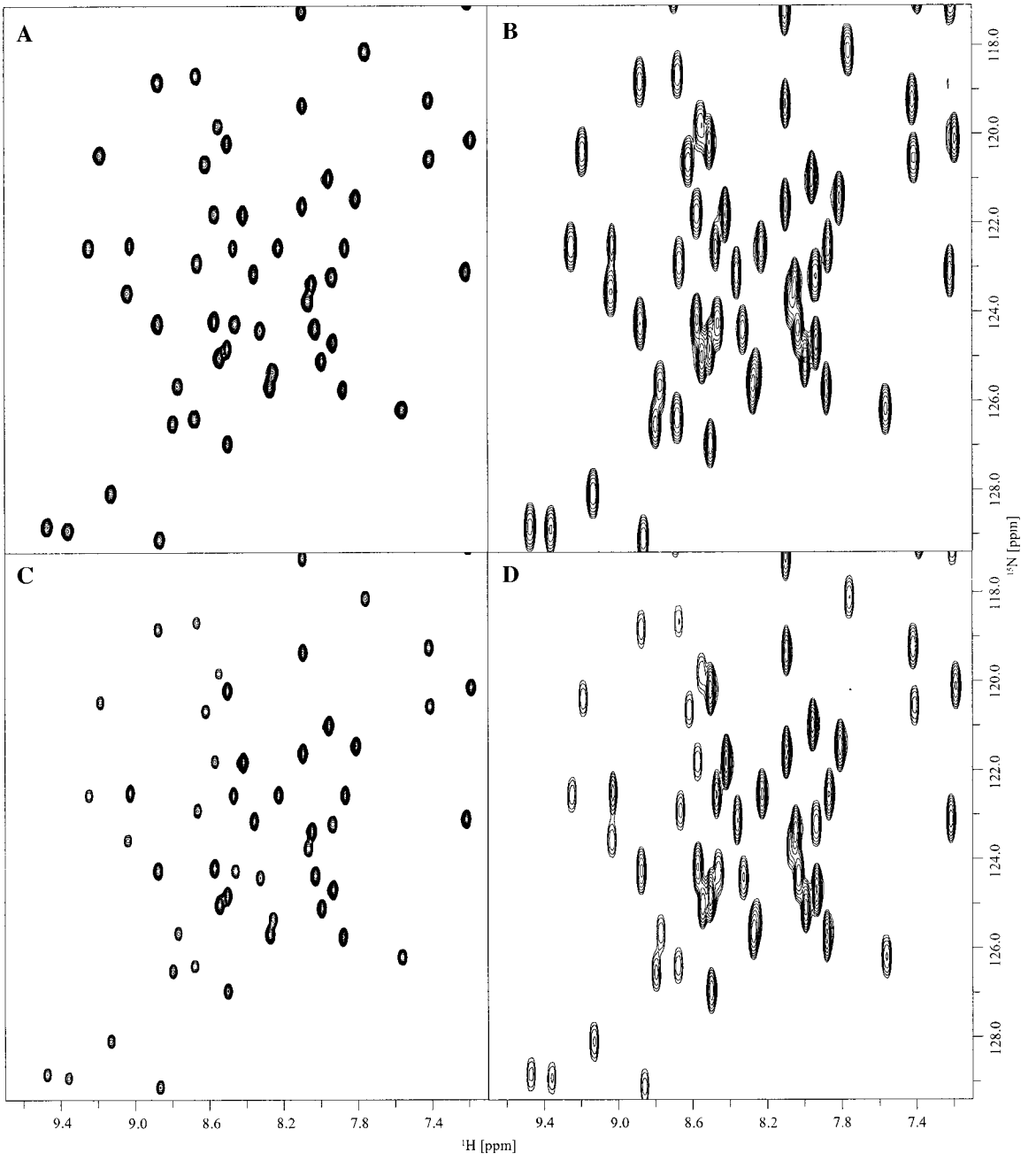

FIG. 2. Comparison between expansions of the 500-MHz spectra of the decoupled SCT-HMSQC-HA (A) and CT-HMQC-HA (B) and corresponding *J*-modulated experiments (C, D), respectively. The data for SCT-HMSQC-HA and CT-HMQC-HA spectra were acquired with $t_{1,\max}$ ($t_{2,\max}$) = 75.3 ms (128 ms) and 28.2 ms (128 ms), respectively, with 64 scans per FID. The time period for *J*-modulation was 40 ms in both experiments. The data were zero-filled to 2k in both dimensions prior to Fourier transform. A phase-shifted squared sine-bell window function was applied in both dimensions of both experiments. The sample contained 1 mM uniformly ^{15}N-labeled ubiquitin (VLI Research Inc. Southeastern, PA) in 90% H_2O, 10% D_2O in a Wilmad 535PP NMR tube, pH 5.8, 50 mM sodium phosphate buffer at 30°C.

gain in resolution in the SCT-HMSQC-HA experiment can clearly be seen in Fig. 2 showing expansions of the ^{15}N–^{1}H correlation maps of the SCT-HMSQC-HA (A, C) and the CT-HMQC-HA (B, D). A small region around the peak tops was integrated for each cross-peak pair in the *J*-modulated and the decoupled experiments, and experimental coupling constants were extracted from the peak volumes using Eq. [1]. The root-mean-square deviation for the $^{3}J_{H^{N}H^{\alpha}}$ couplings measured with the SCT-HMSQC-HA versus the CT-HMQC-HA experiment (Fig. 3) in ubiquitin was 0.40 for the 60 residues considered, i.e., excluding the six glycines, three prolines, and the residues with substantial overlap preventing reliable determi-

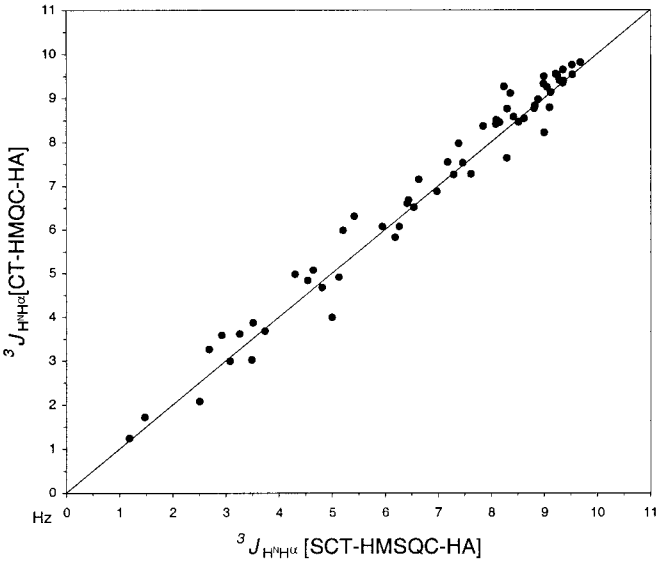

FIG. 3. Correlation of the $^3J_{H^NH\alpha}$ coupling constants measured from ubiquitin with SCT-HMSQC-HA versus CT-HMQC-HA experiments. The pairwise root-mean-squared deviation between these two experiments is 0.40 Hz.

nation of the coupling constants. The individual coupling constants can thus be measured with an accuracy of approximately 0.2 Hz. Obviously, the measurement uncertainty is considerable smaller than the range of coupling constants determined, implying that the proposed method provides reliable $^3J_{H^NH\alpha}$ coupling constants. Also, a comparison of some of the $^3J_{H^NH\alpha}$ coupling constants measured from ubiquitin using the SCT-HMSQC-HA and the CT-HMQC-HA experiments with those found in the literature (*19*) is given in Table 1.

The applicability of the SCT-HMSQC-HA scheme to larger proteins was experimented using the 20-kDa (176 amino acid residues) bacterial protein calerythrin (*20*) (Fig. 4). This calcium-binding protein consists of four helix–loop–helix EF-hand structures and is thus mainly α helical. A $^3J_{H^NH\alpha}$ coupling constant was obtained for 80% of the residues (118 of 146 considered), despite the apparent crowding in the spectrum. In the case of calerythrin, the *J*-modulation period was optimized to coupling values typically found in helices, $T = 50$ ms. Coupling constants of 10 Hz vanish when this long a period of modulation is employed, which explains the disappearance of some cross peaks originating from β strand substructures from the *J*-modulated spectrum. The experimental coupling constants were in good agreement with the known secondary structure (*20*). After correction for effects of differential relaxation (*vide infra*), the α helices gave, to the exclusion of few exceptions, $^3J_{H^NH\alpha}$ values smaller than 6.0 Hz and the short stretches of β strands values greater than 7.5 Hz.

Differential relaxation of the $^1H^N$ in-phase and antiphase magnetization results in a decrease of the apparent $^3J_{H^NH\alpha}$ coupling constants. This phenomenon originates from the rapid $^1H^\alpha$ spin flips and leads to an accelerated relaxation of the antiphase amide proton magnetization compared to that of the in-phase magnetization (*7, 21*). The difference in the relaxation rates of the in-phase and antiphase magnetizations can be estimated to be roughly proportional to the selective longitudinal relaxation rate of the α protons (*13*). If the time period used for the *J*-modulation constitutes a considerable fraction of T_{1,H^α}, a systematic error in the experimental couplings results. It is then obvious that a longer dephasing time period requires a larger correction for the experimental coupling values. Additionally, as R_{1,H^α} increases with increasing protein size, the correction factor needed is larger for larger proteins. Use of a shorter *J*-modulation period is advantageous for large β sheet proteins, since the effects of differential relaxation are smaller, and relatively large coupling constants can be determined accurately. On the other hand, for α helical proteins longer *J*-modulation time periods should be used in order to obtain a reasonable ratio of the cross-peak intensities. The data shown for ubiquitin were not corrected for differential relaxation and are used only to demonstrate the applicability and reliability of the proposed method. Ponstingl and Otting (*16*) provide a thorough discussion on the correction of the differential relaxation in CT-HMQC-HA/HN experiments. Owing to the similarity of the *J*-modulation periods used in both the SCT-HMSQC-HA and the CT-HMQC-HA experiments, the procedure for the correction of the differential relaxation effects introduced by Ponstingl and Otting can be used analogously for the SCT-HMSQC-HA pulse scheme. The coupling constants measured from calerythrin were corrected for effects of differential relaxation by roughly estimating the selective $1/T_{1,H^\alpha}$. Assuming an isotropic rotational correlation time, τ_c, of the order of 7–8 ns for a 20-kDa protein, and that R_{1,H^α} depends nearly linearly on τ_c, an estimate of 8 Hz for R_{1,H^α} was used. This results in a correction factor of 8% ($T = 50$ ms) and, thus, all of the measured coupling constants were multiplied by a factor of 1.08.

In conclusion, we have presented a method which enables

TABLE 1

Comparison between the $^3J_{H^NH^\alpha}$ Coupling Constants Measured from the SCT-HMSQC-HA and the CT-HMQC-HA (*16*) Experiments and the Data for the HNCA-*J* and the HNHA Experiments found in the Literature (*19*)

	$^3J(H^NH^\alpha)$ [Hz]			
Residue	SCT-HMSQC-HA	CT-HMQC-HA	HNCA-*J* (*19*)	HNHA (*19*)
Glu18	9.0	9.4	8.0	8.2
Lys27	3.3	4.1	3.0	3.1
Asp32	2.6	3.2	3.3	3.4
Arg54	8.2	9.2	8.6	8.5
Ile61	6.3	6.1	5.9	6.7
His68	9.2	9.5	9.0	8.9

Note. The coupling values presented are not corrected for effects of differential relaxation.

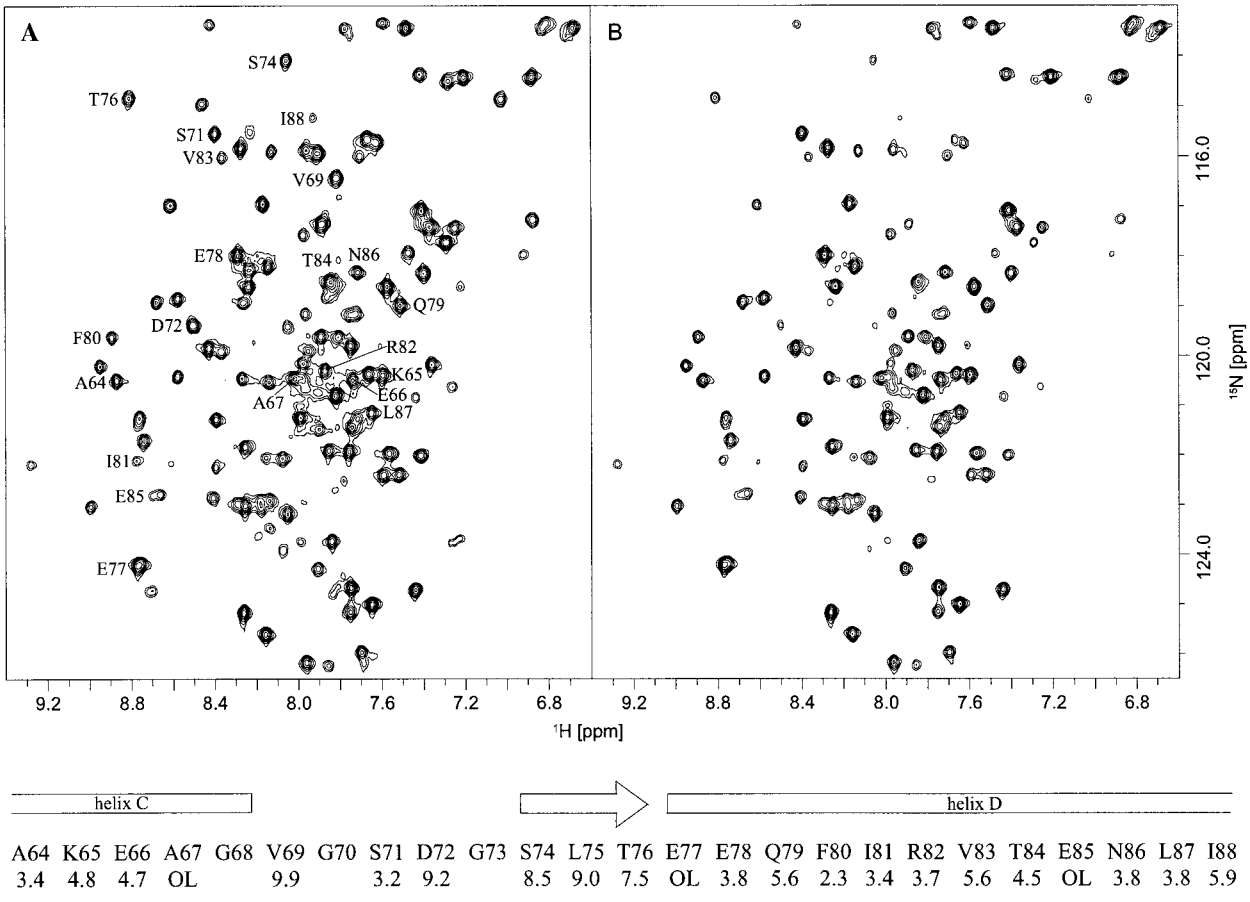

FIG. 4. Representative region from the decoupled (A) and the *J*-modulated (B) SCT-HMSQC-HA spectra of calerythrin. Spectra were recorded at 45°C, at 500-MHz ^{1}H frequency on a Varian Unity 500 NMR spectrometer equipped with a triple-resonance probehead and an actively shielded *z*-axis gradient system. The sample contained 0.75 mM of ^{15}N-labeled calcium-saturated calerythrin (176 residues) in 95% H_2O, 5% D_2O in a 250-μl Shigemi microcell, pH 6.0. Experimental parameters: $T = 50$ ms, $t_{1,\max} = 136$ ms, $t_2 = 128$ ms, recorded with 64 scans per increment. The data were zero-filled to 2k in both dimensions prior to Fourier transform. A phase-shifted squared sine-bell window function was applied in both dimensions. Some residues of the second EF-hand are marked by residue type and number in (A). The $^{3}J_{H^N H^\alpha}$ coupling constants, after correction for effects of differential relaxation, of these residues are listed below the spectra, together with the secondary structure (*20*). Open boxes indicate α helices, arrow represents β strand, and OL denotes overlapping cross peak.

the accurate measurement of $^{3}J_{H^N H^\alpha}$ coupling constants conveniently from a two-dimensional ^{15}N,^{1}H correlation spectrum with high resolution and sensitivity. Owing to the considerably better resolution available in the ^{15}N-dimension, the presented method is also applicable to large (≥20 kDa) or highly helical proteins where resonance overlap is likely to occur frequently. The semi-constant-time approach allows a shorter time period for the *J*-modulation, which improves the sensitivity of the experiment but does not limit the available resolution.

ACKNOWLEDGMENT

This work was supported by the Academy of Finland.

REFERENCES

1. K. Wüthrich, "NMR of Proteins and Nucleic Acids," Wiley, New York (1986).
2. M. Karplus, *J. Chem. Phys.* **30,** 11 (1959).
3. D. Neuhaus, G. Wagner, M. Vasak, J. H. R. Kägi, and K. Wüthrich, *Eur. J. Biochem.* **151,** 257 (1985).
4. L. E. Kay and A. Bax, *J. Magn. Reson.* **86,** 110 (1990).
5. S. Heikkinen, H. Aitio, P. Permi, R. Folmer, K. Lappalainen, and I. Kilpeläinen, *J. Magn. Reson.* **137,** 243 (1999).
6. P. Permi, I. Kilpeläinen, and S. Heikkinen, *Magn. Reson. Chem.* **37,** 821 (1999).
7. A. Rexroth, P. Schmidt, S. Szalma, T. Geppert, H. Schwalbe, and C. Griesinger, *J. Am. Chem. Soc.* **117,** 10389 (1995).
8. P. Schmieder, V. Thanabal, L. P. McIntosh, F. W. Dahlquist, and G. Wagner, *J. Am. Chem. Soc*. **113,** 6323 (1991).
9. M. Görlach, M. Wittekind, B. T. Farmer II, L. E. Kay, and L. Mueller, *J. Magn. Reson. B* **101,** 194 (1993).
10. J. C. Madsen, O. W. Sørensen, P. Sørensen, and F. M. Poulsen, *J. Biomol. NMR* **3,** 239 (1993).
11. R. Weisemann, H. Rüterjans, H. Schwalbe, J. Schleucher, W. Bermel, and C. Griesinger, *J. Biomol. NMR* **4,** 231 (1994).

12. M. Billeter, D. Neri, G. Otting, Y. Q. Qian, and K. Wüthrich, *J. Biomol. NMR* **2,** 257 (1992).
13. G. W. Vuister and A. Bax, *J. Am. Chem. Soc.* **115,** 7772 (1993).
14. H. Kuboniwa, S. Grzesiek, F. Delaglio, and A. Bax, *J. Biomol. NMR* **4,** 871 (1994).
15. A. Meissner, J. Ø. Duus, and O. W. Sørensen, *J. Magn. Reson.* **128,** 92 (1997).
16. H. Ponstingl and G. Otting, *J. Biomol. NMR* **12,** 319 (1998).
17. P. Permi, I. Kilpeläinen, A. Annila, and S. Heikkinen, *J. Biomol. NMR* **16,** 29 (2000).
18. L. E. Kay, P. Keifer, and T. Saarinen, *J. Am. Chem. Soc.* **114,** 10663 (1992).
19. J. Cavanagh, W. Fairbrother, A. G. Palmer III, and N. J. Skelton, "Protein NMR Spectroscopy," Academic Press, San Diego (1996).
20. H. Aitio, A. Annila, S. Heikkinen, E. Thulin, T. Drakenberg, and I. Kilpeläinen, *Prot. Sci.* **8,** 2580 (1999).
21. G. S. Harbison, *J. Am. Chem. Soc.* **115,** 3026 (1993).
22. D. Marion, M. Ikura, R. Tschudin, and A. Bax, *J. Magn. Reson.* **85,** 393 (1989).
23. L. Emsley and G. Bodenhausen, *Chem. Phys. Lett.* **165,** 469 (1990).
24. E. Kupce and R. Freeman, *J. Magn. Reson. A* **105,** 234 (1993).
25. S. H. Smallcombe, S. L. Patt, and P.A. Keifer, *J. Magn. Reson. A* **117,** 295 (1995).